Monitoring of IR Clear-Sky Radiances over Oceans for SST (MICROS)

XINGMING LIANG

NOAA/NESDIS/Center for Satellite Application and Research, Camp Springs, Maryland, and Cooperative Institute for Research in the Atmospheres, Colorado State University, Fort Collins, Colorado

ALEXANDER IGNATOV

NOAA/NESDIS/Center for Satellite Application and Research, Camp Springs, Maryland

(Manuscript received 29 October 2010, in final form 29 March 2011)

ABSTRACT

Monitoring of IR Clear-Sky Radiances over Oceans for SST (MICROS) is a Web-based tool to monitor "model minus observation" (M − O) biases in clear-sky brightness temperatures (BTs) and sea surface temperatures (SSTs) produced by the Advanced Clear-Sky Processor for Oceans (ACSPO). Currently, MICROS monitors M − O biases in three Advanced Very High Resolution Radiometer (AVHRR) bands centered at 3.7, 11, and 12 μm for five satellites, *NOAA-16*, *-17*, *-18*, *-19* and *Meteorological Operational (MetOp)-A*. The fast Community Radiative Transfer Model (CRTM) is employed to simulate clear-sky BTs, using Reynolds SST and National Centers for Environmental Prediction Global Forecast System profiles as input. Simulated BTs are used in ACSPO for improving cloud screening, physical SST inversions, and monitoring and validating satellite BTs. The key MICROS objectives are to fully understand and reconcile CRTM and AVHRR BTs, and to minimize cross-platform biases through improvements to ACSPO algorithms, CRTM and its inputs, satellite radiances, and skin-bulk and diurnal SST modeling.

Initially, MICROS was intended for internal use within the National Environmental Satellite, Data, and Information Service (NESDIS) SST team for testing and improving ACSPO products. However, it has quickly outgrown this initial objective and is now used by several research and applications groups. In particular, inclusion of double differences in MICROS has contributed to sensor-to-sensor monitoring within the Global Space-Based Intercalibration System, which is customarily performed using the well-established simultaneous nadir overpass technique. Also, CRTM scientists have made a number of critical improvements to CRTM using MICROS results. They now routinely use MICROS to continuously monitor M − O biases and validate and improve CRTM performance. MICROS is also instrumental in evaluating the accuracy of the first-guess SST and upper-air fields used as input to CRTM. This paper gives examples of these applications and discusses ongoing work and future plans.

1. Introduction

Developed at the National Environmental Satellite, Data and Information Service (NESDIS), the Advanced Clear-Sky Processor for Oceans (ACSPO) became operational in May 2008 with the Global Area Coverage (GAC) data of the Advanced Very High Resolution Radiometer (AVHRR). As of this writing, ACSPO operational products are generated from *National Oceanic and Atmospheric Administration* (*NOAA*)*-19* and *Meteorological Operational* (*MetOp*)*-A*. Data from back-up satellites *NOAA-16*, *-17*, and *-18* are also processed for cross-platform consistency analyses.

The major ACSPO product is clear-sky radiances over ocean in all AVHRR bands. Sea surfaces temperatures (SSTs) are derived from clear-sky brightness temperatures (BTs) in channel 3B (centered at 3.7 μm), channel 4 (11 μm), and channel 5 (12 μm); and aerosol optical depths are retrieved from clear-sky reflectances in channel 1 (0.63 μm), channel 2 (0.83 μm), and channel 3A (1.61 μm). All three products require validation against known reference data. In ACSPO, expected clear-sky BTs are simulated using the fast Community Radiative Transfer Model (CRTM; Han et al. 2006), similar to the Radiative Transfer Model (RTM) for the Television and Infrared Observation Satellite (TIROS) Operational

Corresponding author address: Xingming Liang, WWB Rm. 603, 5200 Auth Rd., NOAA/NESDIS/STAR, Camp Springs, MD 20746.
E-mail: xingming.liang@noaa.gov

DOI: 10.1175/JTECH-D-10-05023.1

© 2011 American Meteorological Society

Vertical Sounder (RTTOV) (Saunders et al. 1999). Reynolds daily SST (Reynolds et al. 2007) and National Centers for Environmental Prediction (NCEP) Global Forecast System (GFS) upper-air fields are used as input. CRTM BTs are used in ACSPO in conjunction with measured BTs for clear-sky masking (Petrenko et al. 2010) and for exploring improved SST retrievals (Petrenko et al. 2011, manuscript submitted to *Remote Sens. Environ.*). These applications require close agreement between modeled and observed BTs.

CRTM was implemented in ACSPO and preliminarily validated against AVHRR BTs using 1 week of nighttime data (Liang et al. 2009). In this initial implementation, model minus observation (M − O) global biases reached several kelvins. As discussed in Liang et al. (2009), substantial effort was invested into minimizing these large biases, including the treatment of water vapor in CRTM, the improvement to the emissivity model and cloud mask, and the use of Reynolds weekly SST instead of that from NCEP. As a result, in ACSPO version 1, implemented into NESDIS operations in May 2008, all nighttime M − O biases were reduced to only several tenths of a kelvin and are now consistent across platforms to within ~0.1 K. Note that slightly positive bias in the "M" is expected due to missing aerosols in CRTM and the use of bulk (rather than cooler skin) Reynolds SST, which is additionally not corrected for the effect of the diurnal cycle. Also, residual cloud in the AVHRR clear-sky BTs decreases the "O" term, further amplifying the positive shift in the M − O bias.

Customarily, empirical bias correction is performed to reconcile satellite and RTM radiances (e.g., Uddstrom and McMillin 1994; Harris and Kelly 2001; Garand 2003; Köpken et al. 2004; Munro et al. 2004; Merchant et al. 2008, 2009). Empirical bias correction is also employed in ACSPO (Petrenko et al. 2010, 2011, manuscript submitted to *Remote Sens. Environ.*). However, this approach does not address the root causes of the bias, which may result from deficiencies in CRTM or its inputs or errors in sensor calibration and spectral responses. To fully realize the CRTM potential in ACSPO and reduce the need for and reliance upon the empirical bias correction, M − O biases should be constantly monitored, understood, and minimized based on first principles.

Toward this objective, a Web-based diagnostic tool—Monitoring of IR Clear-Sky Radiances over Oceans for SST (MICROS; information online at http://www.star.nesdis.noaa.gov/sod/sst/micros/)—was established to evaluate the M − O BT and regression-minus-Reynolds SST biases in the ACSPO products in near–real time. The MICROS system is described in section 2. Sections 3, 4, and 5 give examples of using MICROS for various applications. Section 6 concludes the paper and discusses ongoing work and future plans.

2. MICROS

a. The major premises of MICROS

In MICROS, differences between observations and their first guesses, Reynolds SST, and corresponding CRTM BTs are monitored. Similar monitoring of M − O biases has been extensively used, for instance, in operational satellite data assimilation in the European Centre for Medium-Range Weather Forecasts (ECMWF; see http://www.ecmwf.int/products/forecasts/d/charts/monitoring/satellite/).

In the climate community, using anomalies (i.e., the deviation of the observation from the expected state) is known to reduce dependency on the nonuniform sample. If first-guess SST and GFS fields are close to reality and CRTM is accurate, then SST and BT biases should be small and characterized by near-Gaussian distribution (Liang et al. 2009; Dash et al. 2010). For accurate cloud masking and SST retrievals in ACSPO, the model should closely match observations. However, nonzero M − O biases of several tenths of a kelvin persist in all AVHRR channels, with corresponding global standard deviations SD ~ 0.4–0.6 K (Liang et al. 2009).

In MICROS, statistical analyses of BT and SST biases are performed in the full clear-sky domain, including the full AVHRR swath ±68°, and all results are displayed with no exemption or additional quality control other than the ACSPO clear-sky mask (Petrenko et al. 2010). Biases are monitored in MICROS in the following several different ways:

1) Global maps of $\Delta T_B = \mathrm{BT_{CRTM}} - \mathrm{BT_{AVHRR}}$ and $\Delta T_S = \mathrm{SST_{AVHRR}} - \mathrm{SST_{Reynolds}}$ are calculated and displayed, along with maps of corresponding geophysical and environmental parameters (water vapor, wind speed, Reynolds SST, air–sea temperature difference, and view and glint angles).
2) Histograms of BT and SST biases are overlaid for five platforms, with their summary daily statistics superimposed (number of observations, mean, and SD).
3) Time series of global daily mean and SD statistics, along with double differences, are used to evaluate the BT and SST biases for cross-platform consistency.
4) Dependencies on the main factors affecting the BT and SST biases—column water vapor content, view zenith angle, wind speed, Reynolds SST, air–sea temperature difference, and latitude—are examined.

In addition to conventional statistics (mean and SD) that are indicative of the overall performance of the ACSPO product, robust statistics [median and robust

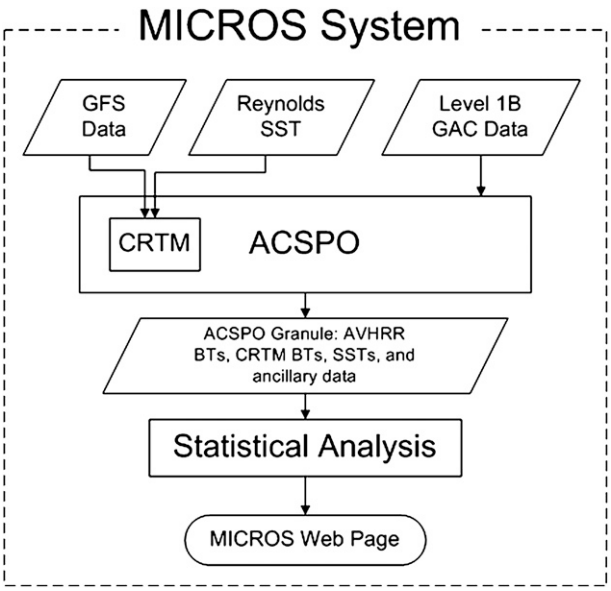

FIG. 1. MICROS flowchart.

standard deviation (RSD)] are also calculated to minimize the effect of possible outliers in ACSPO data on the statistics (cf., Merchant et al. 2008). Outlier-free statistics are particularly useful for validating CRTM and monitoring sensor radiances. Typically, the two statistics closely match, but occasionally they diverge, signaling problems with ACSPO products.

Examples are discussed in upcoming sections; more discussion of the monitoring principles is found in Dash et al. (2010), who document another global monitoring system: the SST Quality Monitor (SQUAM; information online at http://www.star.nesdis.noaa.gov/sod/sst/squam/).

b. Technical implementation

A flowchart of the MICROS system is shown in Fig. 1. MICROS employs ACSPO to process level 1B data and generate product granules, which contain AVHRR and CRTM BTs, retrieved and Reynolds SSTs, cloud mask, solar and sensor view geometries, and additional ancillary data. Once ACSPO 1-h GAC granules have been generated, they are statistically processed in 24-h increments and the results are displayed on the Web. MICROS runs daily and processes global GAC data from five platforms (*NOAA-16–19* and *MetOp-A*). The end-to-end processing takes ~4 h of clock time on a Linux box with four 2.33-GHz processors and 4-GB memory.

All analyses in MICROS are performed separately for day and night. As of this writing, nighttime analyses are more accurate and, therefore, more appropriate for validation of CRTM and satellite radiances, whereas daytime data are less accurate because of the suboptimal treatment of solar reflection in CRTM version 1.1 (Liang et al. 2010). All analyses in this paper are based solely on nighttime ACSPO data.

3. Using MICROS to validate and improve ACSPO products

Since MICROS implementation in July 2008, it proved instrumental to evaluating and testing all new ACSPO developments in near–real time. This section documents results of testing three earlier ACSPO versions, which provided a natural way to estimate the stability and improvements in the ACSPO BT and SST biases.

a. ACSPO versions documented in MICROS

Three ACSPO versions are summarized in Table 1. ACSPO version 1.00 was described in detail in Liang et al. (2009). It employed an alpha version of CRTM (termed r577) in conjunction with Reynolds weekly 1° optimum interpolation SST (OISST version 2; see Reynolds et al. 2002) and an initial version of the ACSPO cloud mask (B. Petrenko et al. 2008, unpublished manuscript).

In ACSPO version 1.02, implemented in MICROS on 4 September 2008, three critical changes were made. First, weekly 1° Reynolds OISST version 2 was replaced with a more accurate daily 0.25° product (Reynolds et al. 2007), which is based on blending the Naval Oceanographic Office (NAVOCEANO) AVHRR SST product (May et al. 1998) with in situ SST. Hereafter, this product is termed Reynolds daily (AVHRR). Another Reynolds daily product that additionally uses SST data from the Advanced Microwave Scanning Radiometer (AMSR) on board the *Aqua* satellite was also tested but did not show improvements in the BT and SST biases. Another critical update in ACSPO version 1.02 was replacing CRTM r577 with the official CRTM version 1.1. Finally, the more accurate transmittance coefficient data for the wide AVHRR bands were used—referred to as the Planck-weighted (PW) coefficients (e.g., Chou et al. 1993; Turner 2000)—instead of the "ordinary" coefficients employed in CRTM r577.

ACSPO version 1.10 was implemented on 3 January 2009. It employed improved clear-sky detection by using flexible band and sensor-specific tests (Petrenko et al. 2010). Also, the threshold at which the day–night flag switches over was changed from a solar zenith angle (SZA) of 85° (in ACSPO versions 1.00 and 1.02) to 90° (in version 1.10).

Below we focus on evaluating the effect of these changes on global BT and SST biases. Also, out-of-family behavior of *NOAA-16* is discussed.

b. Effect of using daily Reynolds SST as CRTM input

Figures 2a,b show that using more accurate daily SST reduces global variance (the square of SD) of ΔT_B

TABLE 1. Different versions of ACSPO employed in MICROS.

	ACSPO version 1.00	ACSPO version 1.02	ACSPO version 1.10
Time interval	1 Jul 2008–3 Sep 2008	4 Sep 2008–11 Nov 2008	12 Nov 2008–10 Oct 2009
Official version	Yes	No	Yes
CRTM version	R577	Version 1.1	Version 1.1
Channel 3B coefficients	Ordinary	Planck weighted	Planck weighted
SST input to CRTM	Reynolds weekly 1° OISST version 2	Reynolds daily 0.25° (''AVHRR'')	Reynolds daily 0.25° (''AVHRR'')
Cloud mask	B. Petrenko et al. (2008, unpublished manuscript)	Petrenko et al. (2010)	Petrenko et al. (2010)
Day/night flag (solar zenith angle)	85°	85°	90°

by almost half, and a corresponding reduction is also observed in ΔT_S (not shown). Importantly, cross-platform consistency of BT and SST biases is also improved. A warm shift of $\sim+0.08$ K in BTs is due to an offset between weekly and daily Reynolds products on the day analyzed here (12 July 2008). A corresponding cold shift (~-0.1 K) is observed in the retrieved-minus-Reynolds SST (not shown). Note that although both weekly and daily Reynolds SST products are anchored to in situ SST, small differences between them are possible, especially as the offset increases from the center of the weekly product centered on Wednesdays (note that 12 July 2008 was a Saturday). Figures 3a,b show that the improvements in the M − O bias are more noticeable in higher latitudes and in some coastal areas. Although more stable and spatially coherent ΔT_B should favorably affect the ACSPO cloud mask, Figs. 2 and 3a,b suggest that the clear-sky ocean domain did not change much, indicating that the ACSPO mask is robust with respect to the first-guess SST field. Figures 4a,b additionally show that the amplitude of the view zenith angle (VZA) dependencies remains largely unchanged. However, different platforms are clustered together more tightly now, likely due to improved spatial and temporal resolution in the daily (1 day × 0.25°) product compared to its weekly (1 week × 1°) predecessor.

c. *Effect of CRTM updates on ACSPO BTs*

Figures 2c–4c show the same dataset as in Figs. 2b–4b but processed with the new CRTM version 1.1 formulation together with Planck-weighted coefficients. For this sensitivity check, the same daily Reynolds SST was used. The clear-sky coverage slightly increases, as is manifested by the larger N values in Fig. 2c. The mean ΔT_B biases are now reduced by ~-0.08 K, thus offsetting the positive shift of $\sim+0.08$ K that occurred as a result of using daily SST. The SDs did not change much. Additional analyses suggest that this change in CRTM BTs is mainly due to using Planck-weighted instead of ordinary coefficients.

Change from CRTM r577 to version 1.1 affected *NOAA-16* channel 3B in a very unique way, which was subject of a separate analysis (Liu et al. 2009). Based on this analysis, treatment of upper-atmospheric layers above 10 mbar in CRTM was revisited. As a result, the M − O bias in *NOAA-16* channel 3B has increased by $\sim+0.3$ K, and the corresponding SD is significantly improved.

d. *Effect of improving clear-sky mask on ACSPO BTs*

Since clear-sky BTs are obtained from a cloud screening algorithm, MICROS can also be used to validate and improve ACSPO clear-sky mask (e.g., Petrenko et al. 2010), including the impact of undetected aerosols (Liang et al. 2009).

The dataset used in Figs. 2c–4c was reprocessed using ACSPO version 1.10, and results are shown in Figs. 2d–4d. Compared to version 1.02, the number of clear-sky observations at night has significantly reduced, mainly due to the change in the day–night threshold in ACSPO version 1.10, from SZA = 85° to SZA = 90°. This reduction is only partly compensated by the increase in the daytime sample size resulting from the additional updates in the cloud mask (Petrenko et al. 2010). Global mean BT and SST biases and their corresponding SDs have consistently reduced in ACSPO version 1.10, and so did the amplitudes of their VZA dependencies, indicating that changes in the ACSPO clear-sky mask had a favorable impact on data of all platforms, except *NOAA-16*.

Quantitative analysis of the aerosol impact on the M − O bias is currently underway and has led to the development of an Aerosol Quality Monitoring (AQUAM; http://www.star.nesdis.noaa.gov/sod/sst/aquam/) Web site. AQUAM is expected to fine-tune the clear-sky mask by improving the aerosol quality

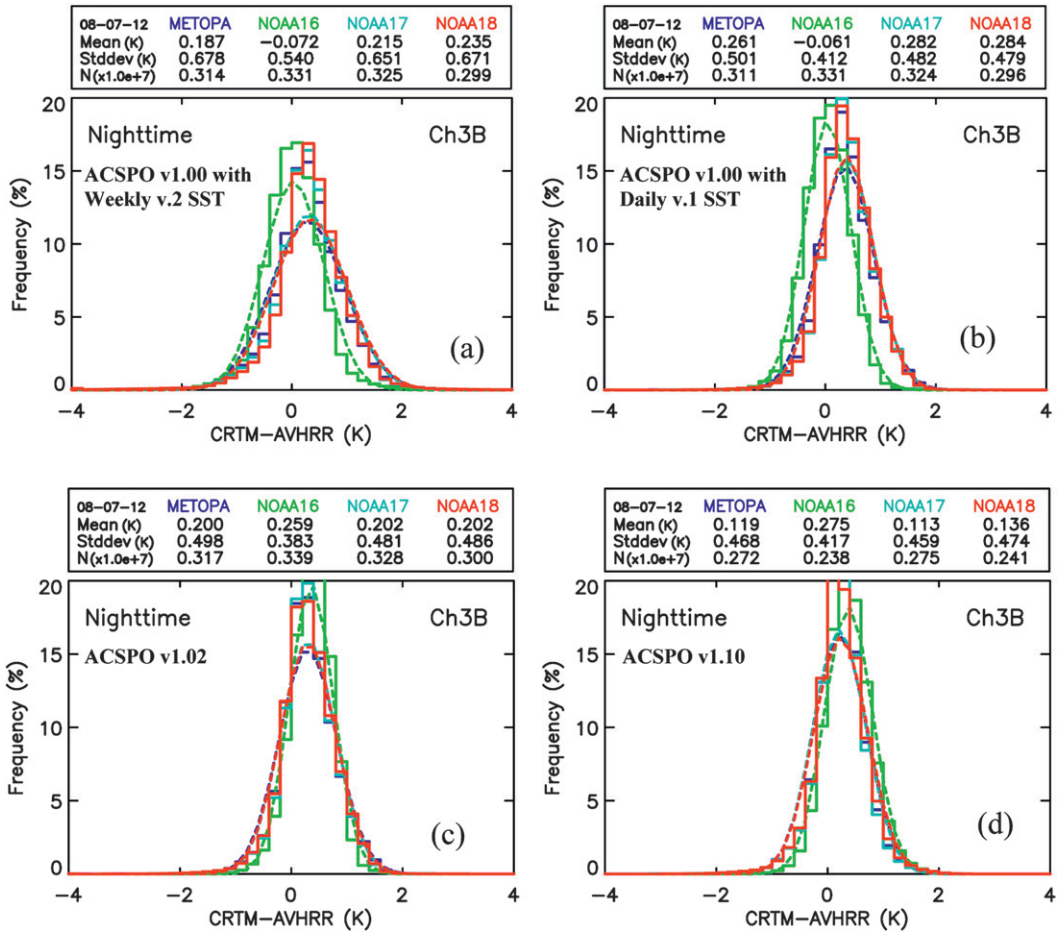

FIG. 2. Global histograms of the M − O BT biases in AVHRR channel 3B on board *MetOp-A* and *NOAA-16–18* for 24 h of nighttime data for 12 Jul 2008. ACSPO version 1.00 with (a) Reynolds weekly 1° version 2.0 SST and (b) Reynolds daily 0.25° version 1.0 SST (AVHRR based) as CRTM input (CRTM r577 was used in both cases); (c) ACSPO version 1.02 [as in (b), but using CRTM version 1.1 and Planck-weighted CRTM coefficients]; and (d) ACSPO version 1.10 [as in (c), but using upgraded cloud mask]. Gaussian distributions corresponding to the mean and standard deviation are shown (dotted lines).

flag. This work is to be the subject of a separate publication.

e. Time series of BT and SST biases

Time series of the mean BT and SST biases are shown in the left panels of Fig. 5. Note that all of the data in Fig. 5 are smoothed by a 7-day moving averaging filter to further suppress noise in the data and rectify the cross-platform signal. *NOAA-19*, launched on 6 February 2009, was added to MICROS monitoring on 23 February 2009 as soon as its thermal bands were commissioned and declared operational. On average, BT biases are ~+0.2 K in channel 3B and ~+0.5 K in channels 4 and 5. Physical mechanisms causing these warm biases were discussed in Liang et al. (2009) and reiterated above in section 1. There was no significant change in the mean M − O bias in any band of any platform (except *NOAA-16* channel 3B) when the ACSPO version was upgraded from version 1.00 to version 1.02. This apparent lack of sensitivity is, in fact, due to compensation between two factors that offset each other: using daily Reynolds and PW CRTM coefficients. Also, the BT and SST biases did not change noticeably when ACSPO version 1.10 was introduced, a remarkable result considering a significant adjustment in the ACSPO cloud mask (Petrenko et al. 2010).

Contrary to the warm bias in ΔT_B, retrieved SSTs are biased cold with respect to Reynolds SST by several tenths of a kelvin (Fig. 5g). Because Reynolds SST is anchored to in situ SSTs (Reynolds et al. 2007), the global mean ACSPO-minus-Reynolds SST bias is a close proxy for the ACSPO minus in situ SST bias. In the initial

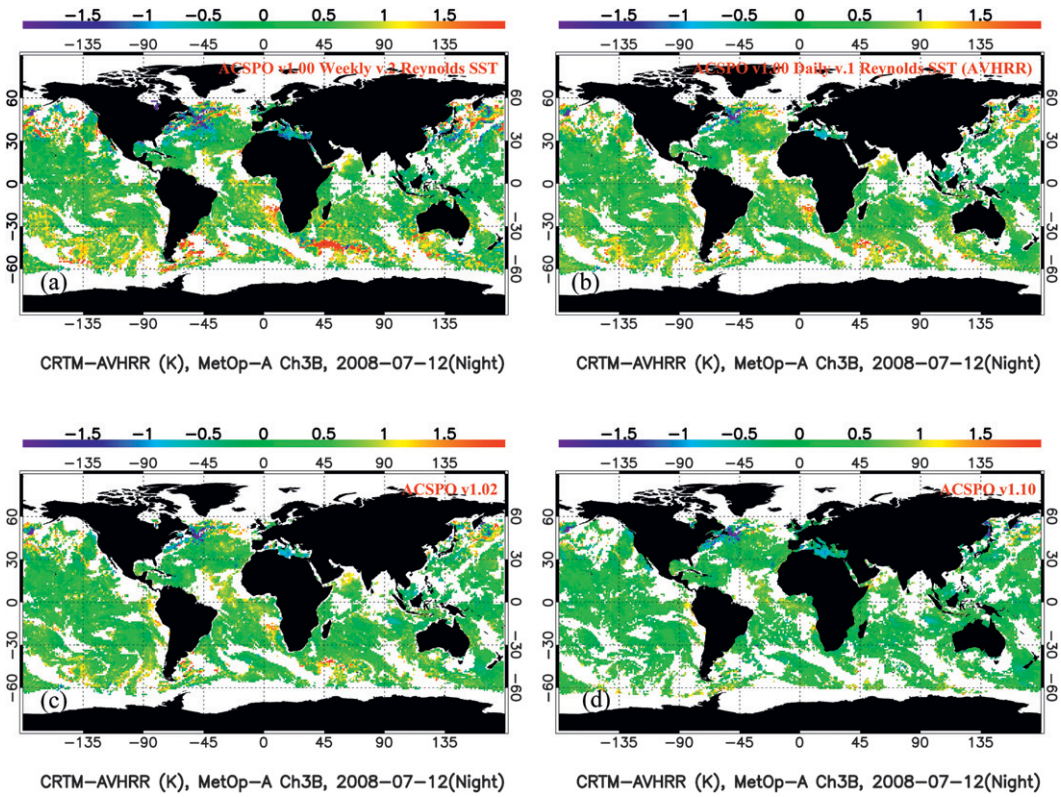

FIG. 3. As in Fig. 2, but for geographical distribution of the M − O BT biases in *MetOp-A* channel 3B.

ACSPO versions discussed here, the SST formulation was intentionally preserved from the NESDIS heritage SST system—the Main Unit Task (MUT; McClain et al. 1985; Ignatov et al. 2004)—for quick cross evaluation of the two SST products. At night, the following triple-window multichannel SST (MCSST) equation is employed:

$$T_s = a_0 + a_1 T_{3b} + a_2 T_4 + a_3 T_5 + [a_4(T_{3b} - T_5) + a_5](\sec\theta - 1). \quad (1)$$

The SST coefficients (a_0, a_1, a_2, a_3, a_4, and a_5) in ACSPO have been adopted from MUT without change (Dash et al. 2010). However, nighttime BTs in MUT are biased warm with respect to ACSPO BTs because MUT selects the warmest clear-sky AVHRR pixel within a collocated High-Resolution Infrared Radiation Sounder (HIRS) footprint, whereas ACSPO processes all clear-sky pixels and does not subsample. Deriving coefficients against warm-biased MUT BTs and using them in an all-clear-sky pixel ACSPO system results in cold-biased ACSPO SSTs. Note that the SST Quality Monitor page (online at http://www.star.nesdis.noaa.gov/sod/sst/squam/ACSPO/acspo_pixel_level_timeseries.htm) also shows a cold bias in nighttime ACSPO SSTs.

The right panels of Fig. 5 show corresponding global SDs. Unlike the global mean biases, the SDs of both ΔT_B and ΔT_S were significantly reduced (from 0.8 to 0.5 K in SST, from 0.7 to 0.5 K in channel 3B, from 0.72 to 0.55 K in channel 4, and from 0.75 to 0.65 K in channel 5) when ACSPO was upgraded from version 1.00 to version 1.02. This is mainly due to using a more accurate daily instead of weekly SST field. As stated in Reynolds et al. (2007), Reynolds SSTs are analysis products (not forecasts), and therefore are available for the use in ACSPO in a delayed mode (the next day for the daily product and the next week for the weekly product).

To better understand the improvement from ACSPO version 1.00 to version 1.02, the plots from 1 July to 11 November 2008 are zoomed and superimposed in the upper right of the corresponding panels. Note that each point now represents 1 day and is not smoothed over 7 days to preserve the fine temporal structure. Before 4 September 2008, the global SDs showed a prominent weekly cycle, which is largest in SST, followed by the most transparent channel 3B and then by channels 4 and 5. The corresponding cycles were also observed in the mean ΔT_B and ΔT_S biases (not shown), although they are seen less clearly than in the SDs. This periodicity was an artifact of using weekly Reynolds SST in ACSPO

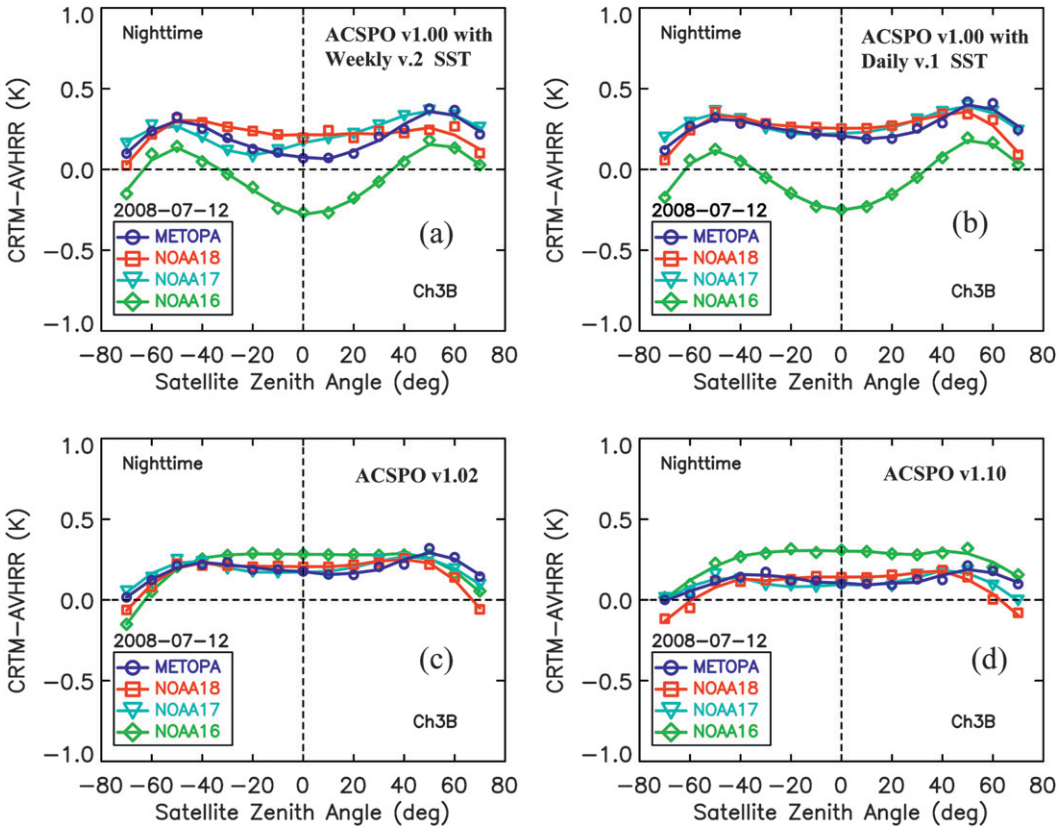

FIG. 4. As in Fig. 2, but for view zenith angle dependencies of the M − O BT biases.

version 1.00, which was resolved when daily SST was employed in ACSPO version 1.02.

f. Anomalous behavior of NOAA-16

NOAA-16 biases are unstable in all bands. This platform currently flies close to the terminator (Liang et al. 2009) and its AVHRR blackbody experiences significant impingement from the solar radiation (Cao et al. 2001, 2004a). This affects calibration in all AVHRR bands, with the largest effect expected in channel 3B. The AVHRR sensor on *NOAA-16* had also experienced continuous problems since September 2003 and has not been used in NOAA operations after *NOAA-18* was launched in May 2005.

In addition to the degraded orbit and unstable sensor, *NOAA-16* channel 3B has shown a consistent cold bias of ~−0.3 K with respect to several AVHRR instruments on board other platforms (Dash and Ignatov 2008; Liang et al. 2009). This anomaly was analyzed in Liu et al. (2009) and found to be due to an out-of-band leak in its spectral response function, which was incorrectly treated in CRTM r577. This problem was fixed in CRTM version 1.1.

Despite these known problems with *NOAA-16*, we have opted to include it in the MICROS monitoring to better understand the performance of the ACSPO system in atypical situations. We believe that *NOAA-16* problems may be corrected. Work with NESDIS calibration colleagues is underway to better understand root causes and to try to mitigate the problems. The current anomalous results will be used as a benchmark to measure future improvements. In the remainder of this paper, *NOAA-16* results will be shown for consistency, but not discussed pending future resolution of its data problems.

Overall, analyses in this section suggest that all of the performance metrics employed in MICROS consistently improved with ACSPO versions.

4. Using MICROS to monitor sensor performance

Global mean biases in Fig. 5 experience day-to-day noise and long-term excursions. These artifacts are coherent between SST and all of the AVHRR bands, and for all platforms. These variations have the largest amplitude in SST, followed by the most transparent channel 3B and then channels 4 and 5. Note, for instance, a strong bump in $\Delta T_B \sim 0.3$ K in channel 3B and ~0.2 K

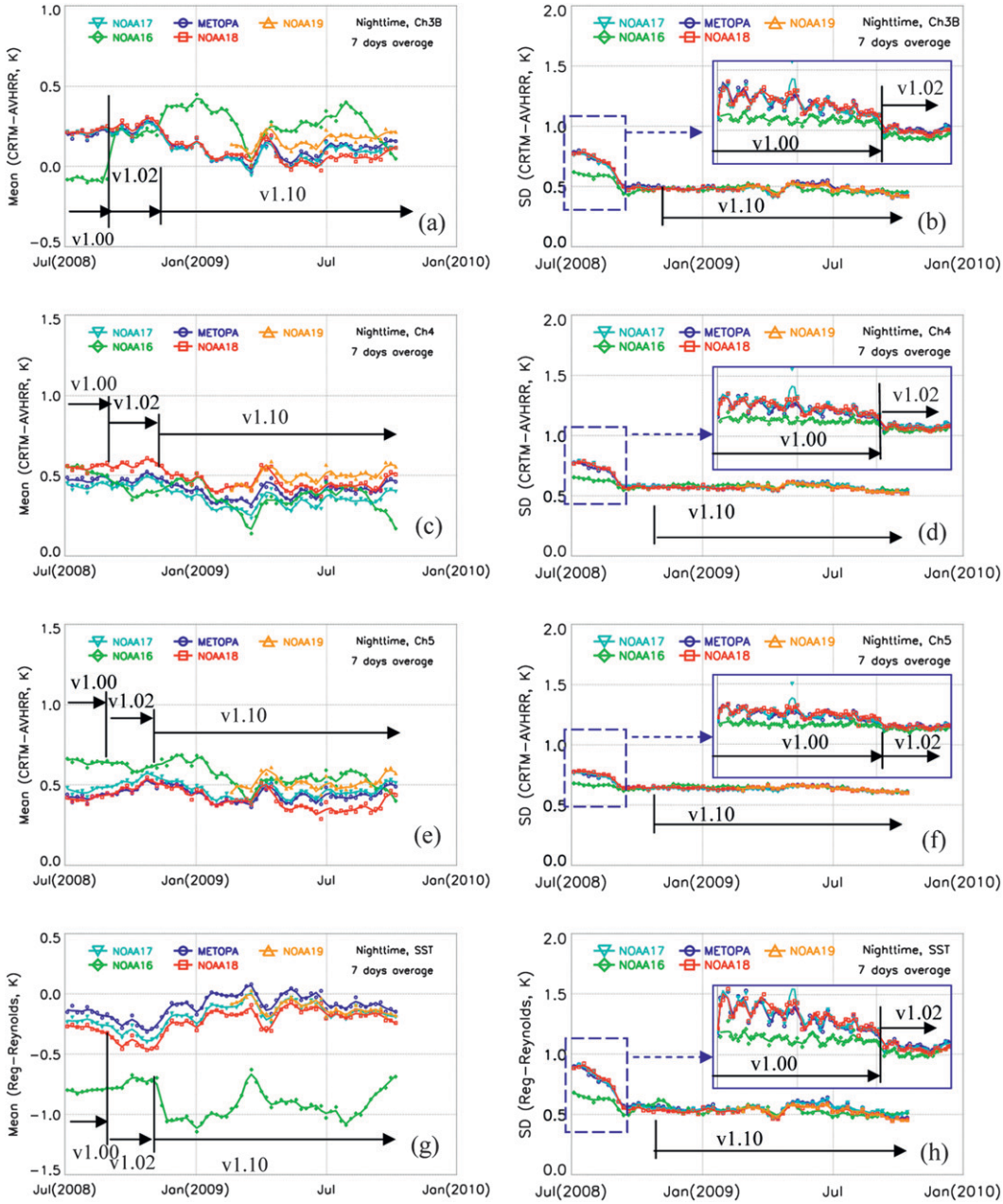

FIG. 5. Time series of the global mean M − O biases and SDs for (a),(b) channel 3B, (c),(d) channel 4, and (e),(f) channel 5, and (g),(h) SST. Each point in the graphs represents the statistics derived from all nighttime data with a 7-day smoothing. ACSPO versions are overlaid. The dashed-line rectangle is magnified in the solid-line rectangle, where nonsmoothed daily data are shown.

in channels 4 and 5 in mid-April 2009, and the several smaller bumps in early January and mid-October 2009. For each BT bump, there is a corresponding hump in ΔT_S. Section 5 will show that these artifacts are caused by spurious variations in Reynolds SST.

Overall, BT biases show high degree of stability and cross-platform consistency, suggesting that calibration and spectral response functions are relatively stable in time. However, spurious variability in data hinders accurate quantitative analyses of the platform-to-platform bias. In MICROS, a double-differencing (DD) technique was adopted to distinguish the cross-platform signal from noise. One platform is designated as the reference (REF), and satellite-to-satellite BT and SST DDs are defined as follows:

$$\mathrm{SAT} - \mathrm{REF} = \mathrm{SAT}[-(M - O)] - \mathrm{REF}[-(M - O)], \quad (2)$$

$$\mathrm{SST} - \mathrm{REF} = \mathrm{SST}[\mathrm{REG} - \mathrm{REYNOLDS}] - \mathrm{REF}[\mathrm{REG} - \mathrm{REYNOLDS}]. \quad (3)$$

The DD technique has been extensively employed, for instance, to establish a calibration link between the Atmospheric Infrared Sounder (AIRS) and the Infrared Atmospheric Sounding Interferometer (IASI) sensors using the Geostationary Operational Environmental Satellite (GOES; Wang and Wu 2008) or radiative transfer model simulation (L. L. Strow et al. 2008, unpublished manuscript) as a transfer standard, and to establish intercalibration links between the *Terra* and *Aqua* Moderate Resolution Imaging Spectroradiometer (MODIS) instruments using AVHRR/*NOAA-17* as a reference (Wu et al. 2008). Similarly to the L. L. Strow et al. (2008, personal communication) study, CRTM is used in MICROS as a transfer standard. The DD technique minimizes the effects on the BT artifacts that arise from such factors as errors in reference SST or GFS upper-air data, incomplete inputs to CRTM (such as missing aerosol), possible systemic biases in the CRTM forward model, and updates in ACSPO processing algorithms. Furthermore, the effects of all of these factors may change in time. The DD largely cancels out these unknown, uncertain, or unstable factors and is, thus, expected to be more effective in cross-calibrating different sensors.

Figure 6 (left) shows DDs calculated from the corresponding panels in Fig. 5. *NOAA-17* was used as a reference platform. Note that in contrast with the classical application of the DD technique, in MICROS the satellite footprints in the two datasets are not required to be collocated in space and time. The different clear-sky coverage between the two platforms likely contributes to day-to-day noise, but the effect of sampling largely cancels out, resulting from using BT and SST biases (i.e., differences rather than absolute values) in calculating DDs. The time series are further disturbed by other data issues, such as outliers and other gross data errors (e.g., present in *NOAA-16*). The right panels of Fig. 6 replot the left panels but using median statistics. In all cases, median time series are less noisy (cf. the sigma values superimposed in the panels). Using robust statistics is thus preferred for DD analyses, whose objective is to rectify the cross-platform consistency signal while minimizing data noise. Note also that all data in Fig. 6 are shown smoothed by a 7-day moving averaging filter.

Three flat lines represent the mean DD biases to help emphasize cross-platform consistency. *NOAA-17* and *MetOp-A* fly in close orbits (both cross the equator at ~2130 local time (LT). It is, therefore, not surprising to see that their ΔT_Bs are consistent to within several hundredths of a kelvin in all bands. However, agreement between *NOAA-17*, on the one hand, and *NOAA-18* and *-19*, on the other, is generally worse. The latter two "afternoon" satellites cross the equator close to ~0140 and ~0200 LT. Typically, diurnal cooling in SST between 2130 and 0200 LT does not exceed ~0.1 K (e.g., Garand 2003; Stuart-Menteth et al. 2005; Kennedy et al. 2007; Gentemann and Minnett 2008). Nighttime BT biases in all bands and from all platforms are thus expected to be within several hundredths of a kelvin, a little larger in the transparent channel 3B and smaller in the more opaque channels 4 and 5. Clearly, the different bands of *NOAA-18* and *-19* do not follow this expected pattern, suggesting that their spectral response functions likely deviate from those assumed in the CRTM or that the calibration is off. Interestingly, cross-platform biases between *NOAA-18* and *-19* (0.09 K in channel B, 0.04 K in channel 4, and 0.12 K in channel 5) are quite large, although these platforms fly in close orbits. The DDs are also helpful to better quantify the instability in all bands of *NOAA-16*.

Note also that despite good consistency between BTs for *MetOp-A* and *NOAA-17*, their corresponding SSTs significantly differ (by ~0.09 K). This is likely due to suboptimal specification of the regression coefficients in the NESDIS heritage MUT system, which are used "as is" in ACSPO.

The SDs of the DDs σ are also listed in Fig. 6. In addition to being a useful indicator of the stability of the DDs in time, they can be also used to estimate the uncertainties of the respective mean DDs. The standard error of the mean of an ensemble of N measurements is $\sigma/\sqrt{N}$. The time series in Fig. 6 span ~420 days, but the number of independent observations is effectively reduced to $N \sim 60$ by the 7-day averaging. For instance, standard error of the *MetOp-A* minus *NOAA-17* bias in channel 4 is $0.012\ \mathrm{K}/\sqrt{60} \sim 0.0015$ K. The mean DD bias of -0.048 K thus appears statistically significant well beyond a 99% confidence level ($\pm 3\sigma_\varepsilon$). These estimates demonstrate the accuracy potential of the DD technique to estimate cross-platform BT and SST biases.

It is useful to place the DD technique in context of the simultaneous nadir overpasses (SNO; online at http://www.star.nesdis.noaa.gov/smcd/spb/calibration/sno) technique (Cao et al. 2004b; Tobin 2008) that is adopted within the Global Space-based Intercalibration System (GSICS; online at http://www.star.nesdis.noaa.gov/smcd/spb/calibration/icvs/GSICS/index.php). In MICROS, cross-platform consistency is monitored in the full global domain and in the full sensor swath, thus resulting in much larger statistics (~3 million clear-sky nighttime

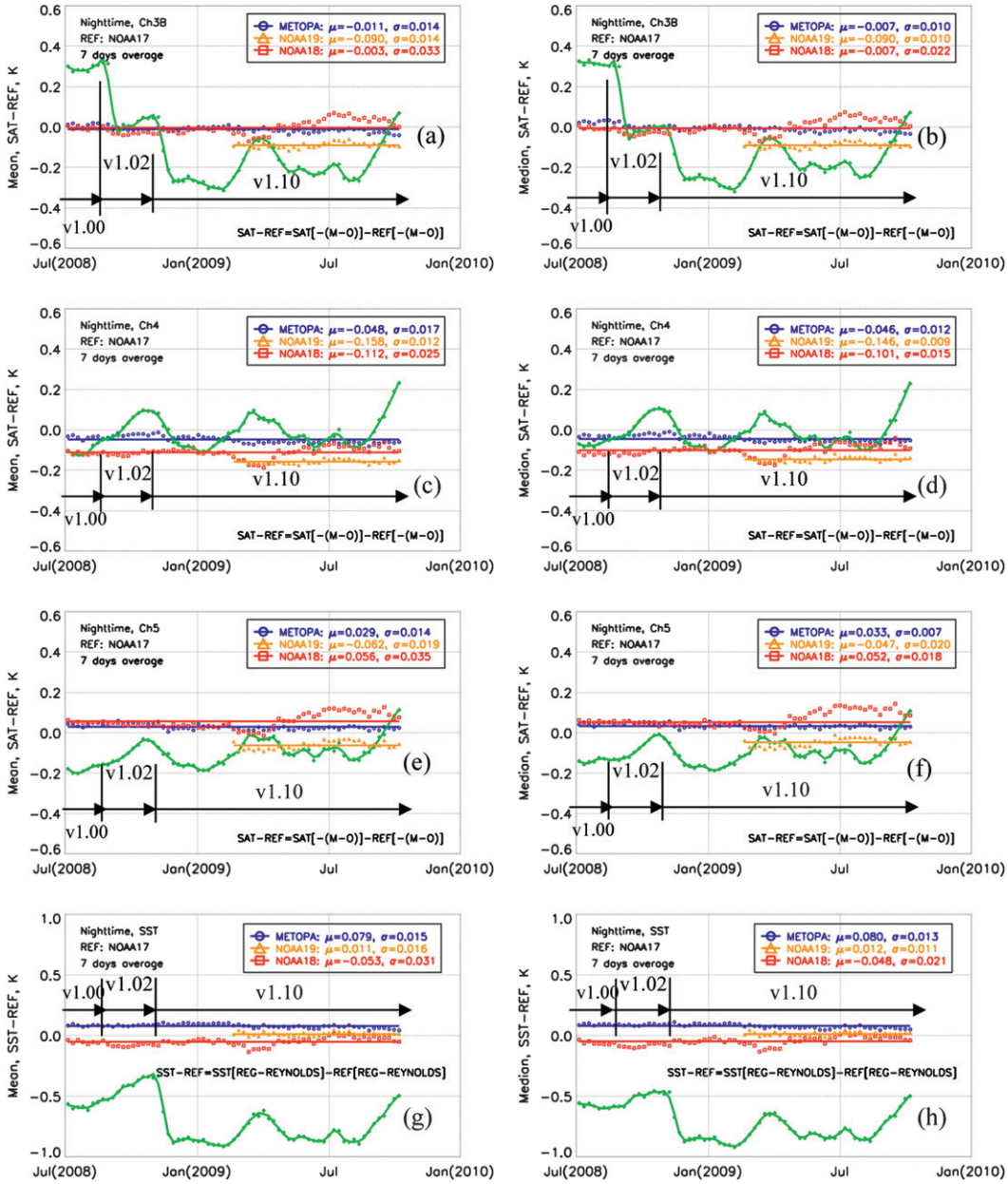

FIG. 6. Cross-platform double differences in AVHRR for (a),(b) channel 3B, (c),(d) channel 4, and (e),(f) channel 5, and (g),(h) SSTs, using (a),(c),(e), and (g) mean and (b),(d),(f), and (h) median statistics. Data are smoothed out by a 7-day moving averaging filter to suppress noise and rectify signal. Mean and median values of the cross-platform biases and their corresponding day-to-day standard deviations are also shown.

pixels per 24-h period), whereas the SNO is based on only a handful of match-up nadir looks per day. Also, DD statistics in MICROS are derived from deviations of clear-sky BTs and SSTs from their respective reference states and follow narrow Gaussian distributions. On the other hand, the SNO statistics are collected in all-sky conditions, in a wide range of illumination geometries, and over different types of underlying surfaces (ice, land, water). As a result, the SNO distributions are wide, strongly asymmetric, and scarcely sampled, making estimates of ensemble mean SNO biases less accurate. Also unique to the DD technique is that it takes into account the difference in spectral response functions between the two sensors, whereas SNO measures a combined effect of sensor calibration and spectral response differences. Finally, because SNOs are mostly collected in the polar

areas, the monitoring of channel 3B (3.7 μm) may be problematic during extended periods of polar days because of solar contamination. As shown in Fig. 6, the DD technique has no problem monitoring this band using nighttime ACSPO data.

Another implementation of the DD technique in GSICS is based on using measured (rather than RTM modeled) high-resolution AIRS or IASI spectra and convoluting them with the sensor spectral response functions (e.g., Hewison and König 2008; Wang and Cao 2008; Wang and Wu 2008). The narrowband sensor and the hyperspectral instrument may be on the same platform [e.g., AVHRR and IASI on *MetOp-A*; see Wang and Cao (2008)], or the two instruments may be flown on different platforms. For example, imagers flown on board the Meteosat Second Generation (MSG) and the *Multifunction Transport Satellite* (*MTSAT*) geostationary satellites are evaluated against collocated IASI on board *MetOp-A* or AIRS on board *Aqua* (Hewison and König 2008; online at http://www.eumetsat.int/Home/Main/DataProducts/Calibration/Inter-calibration/GSICSBiasMeteosatIRInter-calibration/index.htm?l=en, http://mscweb.kishou.go.jp/monitoring/gsics/ir/gsir_mt1r.htm).

Overall, the DD technique employed in MICROS is expected to be an effective supplement to the SNO and spectrometer comparisons methodologies adopted in GSCIS for sensor intercalibration.

5. Using MICROS analyses to validate and improve CRTM and input fields

MICROS analyses have been extensively employed to validate and improve CRTM. Liang et al. (2009) fine-tuned CRTM implementation in ACSPO. Liu et al. (2009) identified a deficiency in treatment of upper-air data in CRTM r577 and fixed it in version 1.1. Section 3b of this paper additionally demonstrated a small yet consistent improvement when PW coefficients were implemented in CRTM version 1.1. Liang et al. (2010) employed MICROS to improve the solar reflectance model. As of this writing, the new and more accurate CRTM version 2 was released to users. More recently, the CRTM team has tested improved transmission parameterizations in wide AVHRR bands, new versions of line-by-line (LBL) RTM, the effects of incorporating additional gases in the training dataset, and the effects of Earth's curvature on M − O biases (Y. Chen and Y. Han 2010, personal communication).

This section additionally demonstrates the value of MICROS to evaluate the effect of input SST field on the M − O biases. Analyses in section 3a have shown that using daily Reynolds SST, instead of the weekly product, greatly improves global SDs between the first-guess BTs and SSTs and the corresponding AVHRR observations. However, time series of BT and SST biases in Fig. 5 continue to exhibit significant and unexplained short- and long-term spurious variations. Furthermore, anticorrelation between BT and SST biases is clearly apparent, suggesting that spurious variability in Reynolds SST is the cause.

To verify this observation, Fig. 7a replots time series of M − O biases in channel 3B from Fig. 5a, zooming at the time interval from 1 January to 30 June 2009, which contained a large wave with the amplitude of several tenths of a kelvin. Note that median statistics are used in Fig. 7 to suppress the unwanted effects of possible outliers in ACSPO data and to emphasize the real trends in M − O biases. Also, unlike Figs. 5 and 6, each data point in Fig. 7 now represents 1-day statistics (i.e., no 7-day smoothing is applied) to preserve day-to-day variations in both datasets. Corresponding temporal median and RSD statistics are superimposed. Typical RSDs are ~33 ± 1 mK. Figure 7b replots Fig. 7a but uses the Met Office 1/20° resolution foundation daily SST product, the Operational Sea Surface Temperature and Sea Ice Analysis (OSTIA; Stark et al. 2007), in place of daily 0.25° Reynolds SST as CRTM input. There is no wave seen in the OSTIA time series, and RSDs have dramatically reduced to ~20 ± 7 mK.

Figures 7c,d show corresponding times series of spatial RSDs calculated within each individual day over the globe. Both Reynolds and OSTIA RSDs show nonuniformities in time with respect to ACSPO SST. The fact that these nonuniformities are specific to Reynolds and OSTIA SSTs and not individual satellite SSTs suggests that they mainly come from these first-guess SSTs rather than from the ACSPO product. On average, RSD ~0.42 K for Reynolds and ~0.32 K for OSTIA, indicating that in addition to being more stable in time, OSTIA also captures spatial SST variability better than the Reynolds product.

Finally, the bottom panels in Fig. 7 compare the corresponding DDs. Nonuniformities in the time series of BTs seen in Figs. 7a,b are expected to cancel out when calculating DDs. Comparisons between Figs. 7e and 7f suggest that indeed this cancellation largely takes place, but artifacts and noise in the DDs are still slightly smaller when OSTIA SST is used. The mean DDs are only slightly affected by the reference SST field.

Figure 8 replots Fig. 7 but for SST biases. All of the observations seen in Fig. 7 continue to hold. The contrast between the Reynolds and OSTIA SSTs is larger than that seen in channel 3B, as expected. With respect to foundation OSTIA SST, ACSPO nighttime SST is biased cold by ~0.15 ± 0.07 K, close to the expected average skin–bulk difference (Donlon et al. 2002). The

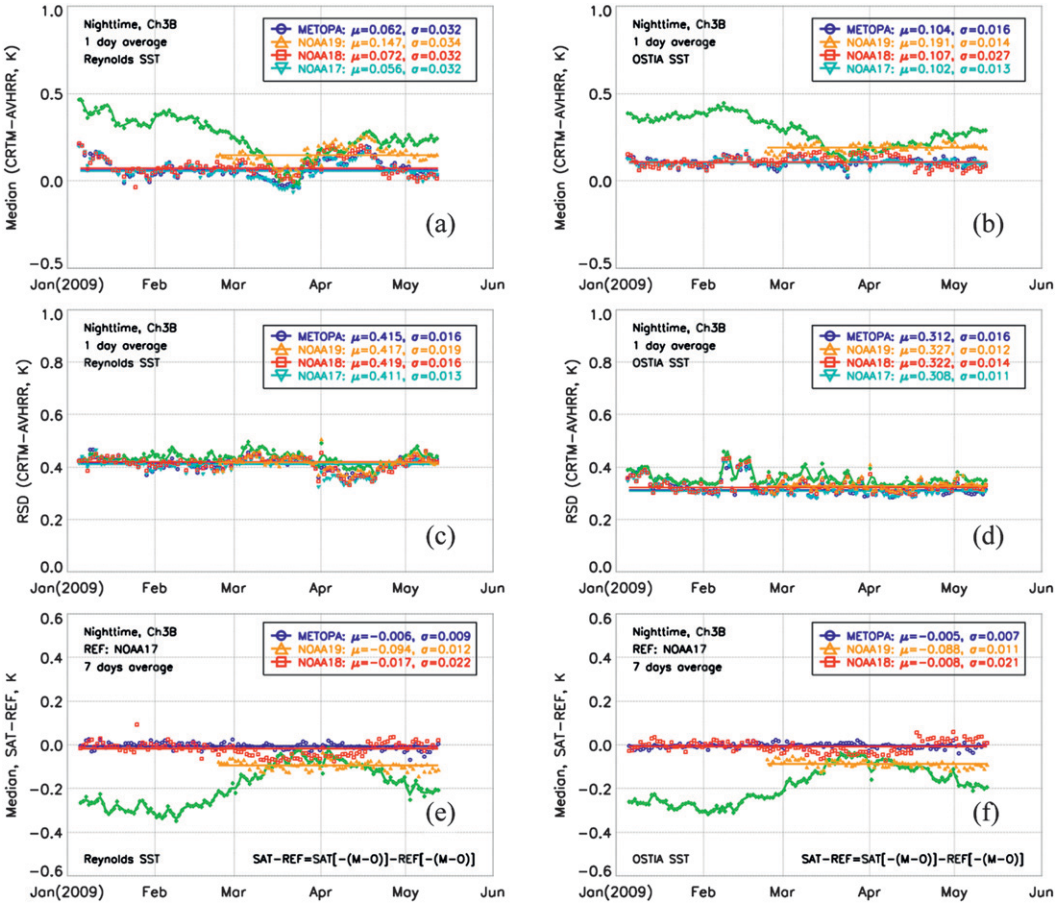

FIG. 7. Time series of the global M − O median (a),(b) BT biases, (c),(d) RSD, and (e),(f) double differences in AVHRR channel 3B for *NOAA-16–19* and *MetOp-A* calculated from ACSPO version 1.10 using (a),(c),(e) Reynolds daily SST and (b),(d),(f) OSTIA SST as CRTM input. Each point in the graphs represents the statistics derived from all nighttime data within a 24-h interval. The superimposed values of μ and σ represent median and RSD statistics derived from individual days.

RSD of ~0.47 K with respect to Reynolds and ~0.35 K with respect to OSTIA clearly indicates reduced spatial noise in the OSTIA SST using ACSPO SST as a "transfer standard." Finally, DDs show that *NOAA-18* SST is ~0.04 K cooler than that of *NOAA-17*, which is expected due to diurnal cycle in SST. However, warm biases in *MetOp-A* and *NOAA-19* SST are unexpected and suggest that MUT regression coefficients are sub-optimal and should be re-derived for ACSPO.

6. Conclusions and future work

The MICROS Web-based tool was established to monitor global M − O biases in clear-sky brightness temperatures and SSTs over oceans in near–real time. MICROS is an end-to-end system that processes satellite level 1B data using ACSPO, performs statistical analyses of BTs and SSTs, and publishes their summaries on the Web. Currently, AVHRR BTs in channels 3B, 4, and 5 from *NOAA-16*, *-17*, *-18*, and *MetOp-A* and regression SSTs are monitored. All analyses in MICROS are performed separately for day and night. Only nighttime data were used in this paper, because they are not contaminated by solar reflectance and are only minimally affected by the diurnal cycle.

Generally, BT and SST biases are stable in time, even when ACSPO versions change. Residual short-term variations mostly arise from the instabilities in CRTM input fields, such as Reynolds SST. Using OSTIA SST as input significantly improves stability of BT and SST time series and reduces spurious spatial variability.

Cross-platform consistency is monitored using double differences. Typically, cross-platform biases are within several hundredths of a kelvin. These biases appear small, but in many cases they are statistically significant. Often, their magnitudes and signs are inconsistent with those

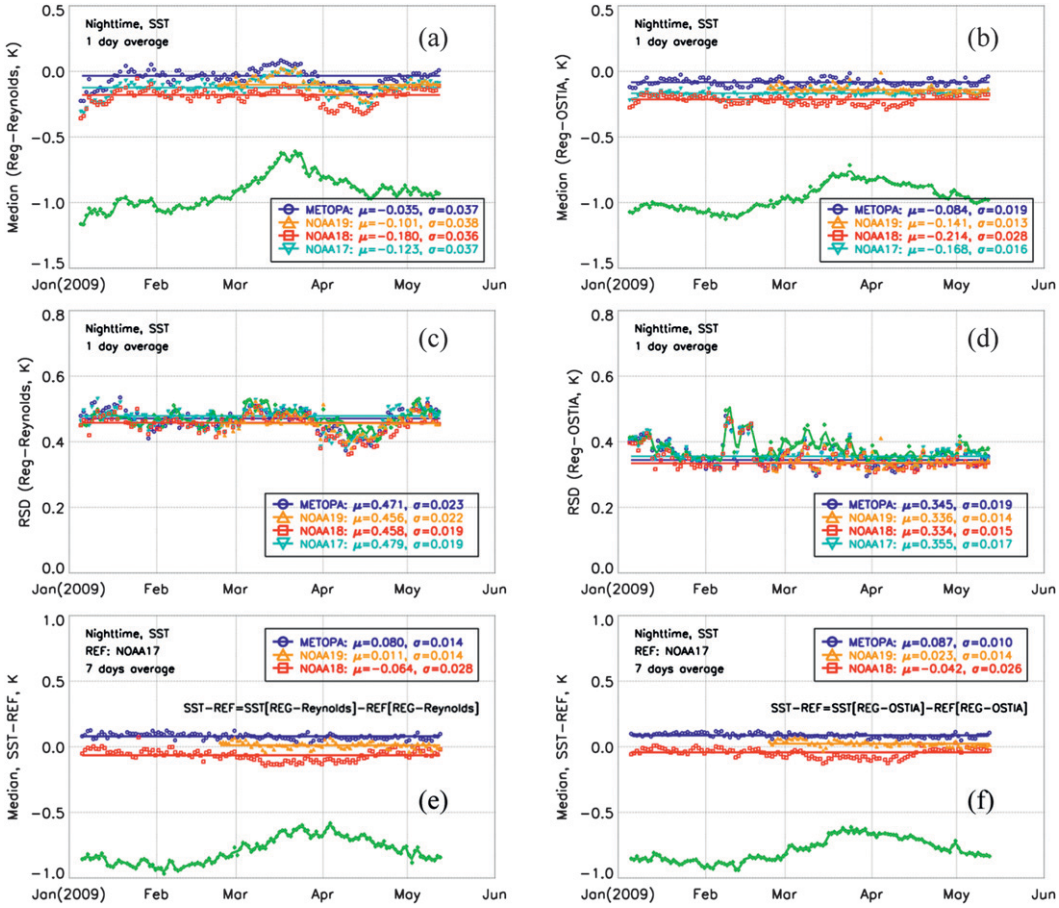

FIG. 8. As in Fig. 7, but for global SST biases.

expected based on diurnal variability (which is not accounted for in MICROS). In some cases the biases are quite large, such as in channels 4 in *NOAA-18* and *NOAA-19*, which are biased cold relative to *NOAA-17* and *MetOp-A* by ~(0.10 ± 0.03) K and ~(0.14 ± 0.01) K, respectively. *NOAA-16* is out of family and unstable.

Both conventional and robust statistics are implemented in MICROS. Robust statistics are more effective for evaluating the performance of the sensor or CRTM and its input, whereas the conventional statistics are useful for evaluating the performance of the ACSPO product (e.g., Merchant et al. 2008, 2009). Proximity of the two statistics is a good indicator of the product's overall well being.

MICROS analyses revealed the need for improvement in several major areas. Daytime BTs are contaminated by the reflected solar signal, especially in the mid-IR channel 3B. Improved and physically justified surface reflectance model based on Cox–Munk formulation was implemented in CRTM version 2 (Liang et al. 2010). It is now being tested and fine-tuned, and the results will be reported elsewhere. Satellite radiances should be reconciled by using the double-differencing technique, improving sensor radiances (calibration and spectral response functions), and accounting for the diurnal variability. We work closely with the CRTM team to explore global model aerosol fields [Goddard Chemistry Aerosol Radiation and Transport (GOCART) and Navy Aerosol Analysis and Prediction System (NAAPS)], in conjunction with CRTM, to more accurately model top-of-atmosphere (TOA) BTs and minimize M − O biases. The CRTM team constantly works to improve CRTM accuracy, and we keep exploring improved input fields (e.g., OSTIA versus Reynolds SST, and ECMWF upper-air fields instead of GFS). Also, ACSPO SST and cloud mask algorithms are constantly evaluated and revisited. The effect of all of these new improvements and developments is evaluated using the MICROS methodology.

Work is also underway to extend MICROS functionality to include monitoring of BTs from the MODIS instruments on board *Terra* and *Aqua* and MSG Spinning Enhanced Visible and Infra-red Imager (SEVIRI). Data

from the National Polar-orbiting Operational Environmental Satellite System (NPOESS) Visible/Infrared Imager Radiometer Suite (VIIRS) and Geostationary Operational Environmental Satellite (GOES)-R Advanced Baseline Imager (ABI) will be added to MICROS once they become available.

Acknowledgments. This work is conducted under the Algorithm Working Group funded by the GOES-R Program Office, NPOESS Ocean Cal/Val project funded by the joint Polar Satellite System (JPSS) Program Office, and Polar PSDI and Ocean Remote Sensing Programs funded by NESDIS. CRTM is provided by the NESDIS Joint Center for Satellite Data Assimilation (JCSDA). Thanks to Yury Kihai for contribution to the ACSPO granule collection, Feng Xu for helpful suggestions related to Web design, and Boris Petrenko for providing a high-quality ACSPO clear-sky mask. Thanks also go to Quanhua Liu, Yong Han, Yong Chen, Paul Van Delst, Fuzhong Weng, Changyong Cao, Likun Wang, and Nick Nalli of NOAA/NESDIS for helpful discussions.Thanks to two anonymous reviewers of this paper for constructive recommendations. The views, opinions, and findings contained in this report are those of the authors and should not be construed as an official NOAA or U.S. Government position, policy, or decision.

REFERENCES

Cao, C., M. Weinreb, and J. Sullivan, 2001: Solar contamination effects on the infrared channels of the advanced very high resolution radiometer. *J. Geophys. Res.,* **106,** 33 463–33 469.

——, J. Sullivan, E. Maturi, and J. Sapper, 2004a: The effect of orbit drift on the calibration of the 3.7 μm channel of the AVHRR onboard NOAA-14 and its impact on night-time sea surface temperature retrievals. *Int. J. Remote Sens.,* **25,** 975–986.

——, M. Weinreb, and H. Xu, 2004b: Predicting simultaneous nadir overpasses among polar-orbiting meteorological satellites for the inter-satellite calibration of radiometers. *J. Atmos. Oceanic Technol.,* **21,** 537–542.

Chou, M. D., W. L. Ridgway, and M.-H. Yan, 1993: One-parameter scaling and exponential-sum fitting for water vapor and CO_2 infrared transmission functions. *J. Atmos. Sci.,* **50,** 2294–2303.

Dash, P., and A. Ignatov, 2008: Validation of clear-sky radiances over oceans simulated with MODTRAN4.2 and global NCEP GDAS fields against nighttime NOAA15–18 and MetOp-A AVHRRs data. *Remote Sens. Environ.,* **112,** 3012–3029.

——, ——, Y. Kihai, and J. Sapper, 2010: The SST Quality Monitor (SQUAM). *J. Atmos. Oceanic Technol.,* **27,** 1899–1917.

Donlon, C. J., P. J. Minnett, C. Gentemann, T. J. Nightingale, I. J. Barton, B. Ward, and M. J. Murray, 2002: Toward improved validation of satellite sea surface skin temperature measurements for climate research. *J. Climate,* **15,** 353–369.

Garand, L., 2003: Toward an integrated land–ocean surface skin temperature analysis from the variational assimilation of infrared radiances. *J. Appl. Meteor.,* **42,** 570–583.

Gentemann, C. L., and P. J. Minnett, 2008: Radiometric measurements of ocean surface thermal variability. *J. Geophys. Res.,* **113,** C08017, doi:10.1029/2007JC004540.

Han, Y., P. van Delst, Q. Liu, F. Weng, B. Yan, R. Treadon, and J. Derber, 2006: JCSDA Community Radiative Transfer Model (CRTM)—Version 1. NOAA Tech. Rep. NESDIS 122, 40 pp. [Available online at http://www.star.nesdis.noaa.gov/sod/sst/micros/pdf/CRTM_v1_NOAAtechReport-1.pdf.]

Harris, B. A., and G. Kelly, 2001: A satellite bias correction scheme for radiance assimilation. *Quart. J. Roy. Meteor. Soc.,* **127,** 1453–1468.

Hewison, T. J., and M. König, 2008: Inter-calibration of Meteosat imagers and IASI. *Proc. 2008 EUMETSAT Meteorological Satellite Conf.,* Darmstadt, Germany, EUMETSAT. [Available online at http://www.eumetsat.int/idcplg?IdcService=GET_FILE&dDocName=PDF_CONF_P_S2_02_HEWISON_V&RevisionSelectionMethod=LatestReleased.]

Ignatov, A., and Coauthors, 2004: Global operational SST and aerosol products from AVHRR: Current status, diagnostics, and potential enhancements. Preprints, *13th Conf. Satellite Oceanography and Meteorology,* Norfolk, VA, Amer. Meteor. Soc., P5.17. [Available online at http://ams.confex.com/ams/pdfpapers/78049.pdf.]

Kennedy, J. J., P. Brohan, and S. F. B. Tett, 2007: A global climatology of the diurnal variations in sea-surface temperature and implications for MSU temperature trends. *Geophys. Res. Lett.,* **34,** L05712, doi:10.1029/2006GL028920.

Köpken, C., G. Kelly, and J.-N. Théapaut, 2004: Assimilation of Meteosat radiance data within the 4D-Var system at ECMWF: Assimilation experiments and forecast impact. *Quart. J. Roy. Meteor. Soc.,* **130,** 2277–2292.

Liang, X.-M., A. Ignatov, and Y. Kihai, 2009: Implementation of the Community Radiative Transfer Model in Advanced Clear-Sky Processor for Oceans and validation against nighttime AVHRR radiances. *J. Geophys. Res.,* **114,** D06112, doi:10.1029/2008JD010960.

——, ——, Y. Han, and H. Zhang, 2010: Validation and improvements of daytime CRTM performance using AVHRR IR 3.7 μm band. Preprints, *13th Conf. on Atmospheric Radiation,* Portland, OR, Amer. Meteor. Soc., P2.3. [Available online at http://ams.confex.com/ams/pdfpapers/170593.pdf.]

Liu, Q., X. Liang, Y. Han, P. van Delst, Y. Chen, A. Ignatov, and F. Weng, 2009: Effect of out-of-band response in *NOAA-16* AVHRR channel 3b on top-of-atmosphere radiances calculated with the community radiative transfer model. *J. Atmos. Oceanic Technol.,* **26,** 1968–1972.

May, D. A., M. Parmeter, D. Olszewski, and B. McKenzie, 1998: Operational processing of satellite sea surface temperature retrievals at the Naval Oceanographic Office. *Bull. Amer. Meteor. Soc.,* **79,** 397–407.

McClain, E. P., W. G. Pichel, and C. C. Walton, 1985: Comparative performance of AVHRR-based multichannel sea surface temperatures. *J. Geophys. Res.,* **90,** 11 587–11 601.

Merchant, C., P. Le Borgne, A. Marsouin, and H. Roquet, 2008: Optimal estimation of sea surface temperature from split-window observations. *Remote Sens. Environ.,* **112,** 2469–2486.

——, ——, H. Roquet, and A. Marsouin, 2009: Sea surface temperature from a geostationary satellite by optimal estimation. *Remote Sens. Environ.,* **113,** 445–457.

Munro, R., C. Köpken, G. Kelly, J.-N. Théapaut, and R. Saunders, 2004: Assimilation of Meteosat radiance data within the 4DVar system at ECMWF: Data quality monitoring, bias correction,

and single-cycle experiments. *Quart. J. Roy. Meteor. Soc.,* **130,** 2293–2313.

Petrenko, B., A. Ignatov, Y. Kihai, and A. Heidinger, 2010: Clear-sky mask for the Advanced Clear-Sky Processor for Oceans. *J. Atmos. Oceanic Technol.,* **27,** 1609–1623.

Reynolds, R. W., N. A. Rayner, T. M. Smith, D. C. Stokes, and W. Wang, 2002: An improved in situ and satellite SST analysis for climate. *J. Climate,* **15,** 1609–1625.

——, T. M. Smith, C. Liu, D. B. Chelton, K. S. Casey, and M. G. Schlax, 2007: Daily high-resolution blended analyses for sea surface temperature. *J. Climate,* **20,** 5473–5496.

Saunders, R., M. Matricardi, and P. Brunel, 1999: An improved fast radiative transfer model for assimilation of satellite radiances observations. *Quart. J. Roy. Meteor. Soc.,* **125,** 1407–1425, doi: 10.1256/smsqj.55614.

Stark, J. D., C. J. Donlon, M. J. Martin, and M. E. McCulloch, 2007: OSTIA: An operational, high resolution, real time, global sea surface temperature analysis system. *Proc. OCEANS'07 Europe,* Aberdeen, Scotland, IEEE, Paper 061214-029, doi:10.1109/OCEANSE.2007.4302251.

Stuart-Menteth, A. C., I. S. Robinson, and R. A. Weller, 2005: Sensitivity of the diurnal warm layer to meteorological fluctuations. Part 2: A new parameterization for diurnal warming. *J. Atmos. Ocean Sci.,* **10,** 209–234.

Tobin, D., 2008: An SNO analysis of IASI and AIRS spectral radiance. *GSICS Quarterly,* Vol. 2, No. 3, 2–4. [Available online at http://www.star.nesdis.noaa.gov/smcd/GCC/documents/newsletter/GSICS_Quarterly_Vol2No3_2008.pdf.]

Turner, D., 2000: Systematic errors that are due to the monochromatic-equivalent radiative transfer approximation in thermal emission problems. *Appl. Opt.,* **39,** 5663–5670.

Uddstrom, M. J., and L. M. McMillin, 1994: System noise in the NESDIS TOVS forward model. Part I: Specification. *J. Appl. Meteor.,* **33,** 919–938.

Wang, L., and C. Cao, 2008: On-orbit calibration assessment of AVHRR longwave channels on MetOp-A using IASI. *IEEE Trans. Geosci. Remote Sens.,* **46,** 4005–4013.

——, and X. Wu, 2008: GSICS tools used to compare IASI and AIRS. *GSICS Quarterly,* Vol. 2, No. 4, 4. [Available online at http://www.star.nesdis.noaa.gov/smcd/GCC/documents/newsletter/GSICS_Quarterly_Vol2No4_2008.pdf.]

Wu, A., X. Xiong, and C. Cao, 2008: *Terra* and *Aqua* MODIS intercomparison of three reflective solar bands using AVHRR onboard the NOAA-KLM satellites. *Int. J. Remote Sens.,* **29,** 1997–2010.